analytical chemistry

Article

Cite This: Anal. Chem. 2019, 91, 3078−3084

pubs.acs.org/ac

A Reader-Based Assay for m^{6}A Writers and Erasers

Lars Wiedmer, Stefanie Alexandra Eberle, Rajiv Kumar Bedi, Paweł Śledź,* and Amedeo Caflisch*

Department of Biochemistry, University of Zurich, Winterthurerstrasse 190, CH-8057 Zurich, Switzerland

ABSTRACT: We have developed a homogeneous time-resolved fluorescence (HTRF)-based enzyme assay to measure the catalytic activity of N^6-methyladenosine (m^{6}A) methyltransferases and demethylases. The assay detects m^{6}A modifications using the natural m^{6}A-binding proteins (m^{6}A readers). The reaction product or substrate m^{6}A-containing RNA and the m^{6}A reader protein are fluorescently labeled such that their proximity during binding initiates Förster resonance energy transfer (FRET). We show that our HTRF assay can be used for high-throughput screening, which will facilitate the discovery of small-molecule modulators of m^{6}A (de)methylases.

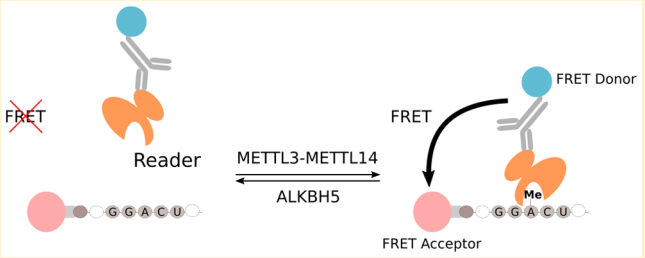

The conversion of adenosine to N^6-methyladenosine (m^{6}A) is one of the most common post-transcriptional modifications in eukaryotic mRNA.[1,2] It often occurs within the DRACH (D = A, G, U; R = A, G; H = A, C, U) consensus motif.[3,4] The m^{6}A level can vary among different tissues and development states or in response to cellular stress.[5,6] The dynamic level of m^{6}A is regulated by the interplay of erasers and writer (Figure 1A). While the writer has been known for two decades,[7] the discovery of m^{6}A-specific eraser proteins FTO (ALKBH9)[8] and ALKBH5[9] has ultimately demonstrated the reversibility of the modification and its regulatory role. In the biological context, FTO mainly acts on N^6,2′-O-dimethyladenosine (m^{6}A$_m$) in the mRNA cap structure rather than m^{6}A.[10] Both m^{6}A demethylases belong to the dioxygenase AlkB family, whose enzymatic reaction depends on Fe(II) and 2-oxoglutaric acid (2OG). The core writer complex is formed by two methyltransferase-like proteins, METTL3 and METTL14, which rely on additional cofactors for mRNA substrate recruitment, including WTAP and RBM15.[4,11,12] The METTL3−METTL14 complex transfers a methyl group from S-adenosylmethionine (SAM) to the adenosine within the consensus sequence of GGACU.[4] Only METTL3 has an intact SAM-binding site, while METTL14 possesses a dysfunctional one.[13−15] The individual depletion of METTL3 or METTL14 reduces the level of m^{6}A in HeLa cells.[4] More importantly, deregulation of METTL3 has recently been linked to specific tumors, such as acute myeloid leukemia,[16] hepatocellular carcinoma,[17] and lung adenocarcinoma.[18] Therefore, the discovery of small-molecule modulators of the METTL3−METTL14 writer has drawn wide attention.[19] Except for the byproduct S-adenosyl-L-homocysteine (SAH),[20] there is no inhibitor reported as of today.

Several ways of monitoring the activity of the m^{6}A writer complex have been reported to date. In their pioneering work in 2014, Liu et al. reported that METTL3 forms a complex with METTL14. They monitored the enzymatic activity of METTL3−METTL14 by quantifying the amount of methylated product through LC/MS/MS analysis.[4] This method is laborious and time-consuming and therefore not suitable for application in inhibitor screenings. The radioactivity-based assay using a radiolabeled methyl group for m^{6}A formation has followed.[14,15,20,21] This approach was more convenient, and Li et al. showed that this format is compatible for high-throughput screening (HTS) with a Z′-factor of 0.78.[20] To avoid the use of radioactive materials, one of us had previously developed an enzyme-linked immunosorbent assay (ELISA) that employs the m^{6}A-specific antibodies for the detection of the modification,[13] which suffered from high background signal and was not suitable for HTS applications. Furthermore, radioactivity- and ELISA-based approaches require multiple washing steps and/or special equipment. Noteworthy, the coupled assay combining the methyl transfer with the MazF RNase specific for unmodified RNA has also been reported.[22] Nevertheless, the use of this coupled assay in high-throughput has not been shown.

Here we report a new assay for the m^{6}A writer activity. To improve the detection system and avoid the limitations of the m^{6}A-specific antibody-based detection, we have explored the application of the YT521-B homology (YTH) protein domain for quantifying the level of produced m^{6}A modification. The human genome carries five m^{6}A readers, namely, YTHDC1, YTHDC2, YTHDF1, YTHDF2, and YTHDF3, four of which are used herein. These protein domains are the natural readers of m^{6}A-modified RNA, as they selectively recognize m^{6}A within the consensus sequence of GG(m^{6}A)CU.[23−25] Recently, it has been shown that they can also bind to N^1-methyladenosine (m^{1}A).[26] To quantify the interaction between modified RNA and its reader, we use the assay technology based on homogeneous time-resolved fluorescence (HTRF). In short, the Eu^{3+}-labeled antibody (HTRF donor)

Received: November 28, 2018
Accepted: January 21, 2019
Published: February 4, 2019

DOI: 10.1021/acs.analchem.8b05500
Anal. Chem. 2019, 91, 3078−3084

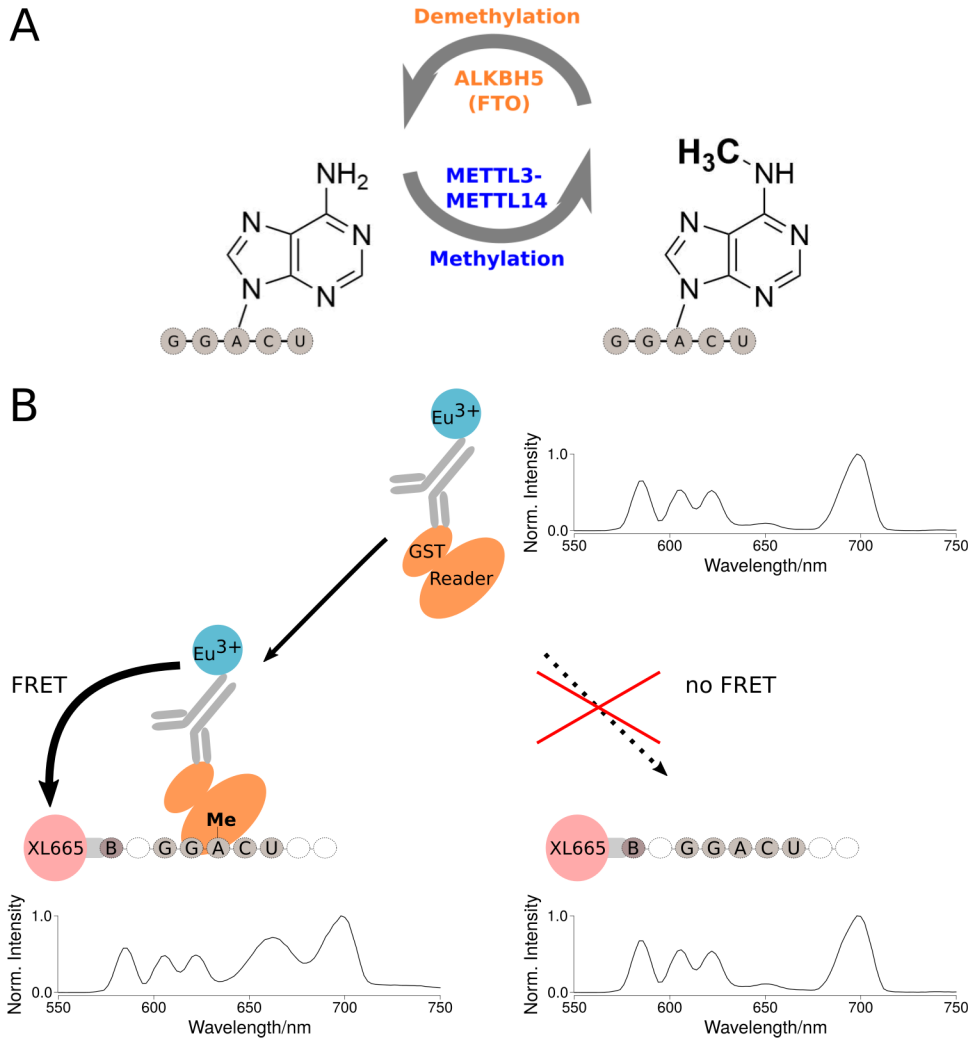

Figure 1. Detection of the reversible m^{6}A modification. (A) Modifying enzymes of N^6-methyladenosine (m^{6}A) include writer (methyltransferase complex: METTL3−METTL14) and erasers (demethylases: ABLKH5 and FTO). These enzymes methylate or demethylate the adenosine within the GGACU consensus sequence. FTO is written in parentheses because of its potentially subordinated role in m^{6}A modifications in the cell.[10] (B) Reader proteins recognize the modification of m^{6}A. An antibody labeled with Förster resonance energy transfer (FRET) donor (europium (Eu^{3+})) binds to the reader at its purification tag, glutathione S-transferase (GST). The biotinylated RNA, in turn, carries the FRET acceptor (XL665) through the streptavidin−biotin interaction. The binding between the methylated RNA and the m^{6}A reader brings the fluorophores in close proximity such that they can undergo FRET. This effect leads to an additional energy transfer peak at around 665 nm in the emission spectrum. Emission spectra are shown for the Eu^{3+}-labeled antibody bound to the $YTHDC1_{345-509}$ itself and in the presence of m^{6}A-containing or unmodified RNA, both labeled with the FRET acceptor. The excitation wavelength was set to 317 nm, and the intensities were normalized to the highest common peak at 698 nm.

binds to the readers by recognizing the affinity tag, glutathione S-transferase (GST). The biotinylated RNA, in turn, is marked by the biotin−streptavidin interaction with the XL665-conjugated streptavidin (HTRF acceptor). The binding between methylated RNA and m^{6}A reader brings the fluorophores in close proximity for Förster resonance energy transfer (FRET) (Figure 1B). We show that this detection system can be used to quantify the amount of m^{6}A after the reaction catalyzed by the methylase METTL3−METTL14 and also to monitor the depletion of m^{6}A-containing RNA in the reaction catalyzed by the eraser ALKBH5.

METHODS

Protein Expression and Purification. We used truncated constructs of the m^{6}A readers comprising the m^{6}A-recognition domain (i.e., the YTH domain). In this regard, the DNA sequences encoding the human YTH domains ($YTHDC1_{345-509}$, $YTHDF1_{361-559}$, $YTHDF2_{383-579}$, $YTHDF3_{391-585}$) were amplified and cloned into the pGEX-6P-1 vector using the restriction sites BamH1 and Xho1. The amplification templates were a gift from Cheryl Arrowsmith, Markus Landthaler, and Chuan He (Addgene plasmids # 64652, 64653, 38089, 70088).[27,28] All the domains were overexpressed in Rosetta (DE3) cells upon induction with 100 μM isopropyl thio-beta-D-galactoside (IPTG) for 20 h at 18 °C. Harvested cells were lysed in 50 mM sodium phosphate at pH 7.2, 150 mM NaCl, 1 mM 1,4-dithiothreitol (DTT), 1 mM phenylmethylsulfonyl fluoride (PMSF), and 1 mM ethylenediaminetetraacetic acid (EDTA) buffer by sonication. After centrifugation at 18 000 rpm at 4 °C for 1 h, the soluble proteins were loaded onto a column packed with glutathione sepharose 4B (GE Healthcare) and subsequently eluted with 10 mM reduced glutathione in buffer containing 50 mM Tris-HCl, pH 8.0, 150 mM NaCl, and 1 mM DTT. Finally, a size-

DOI: 10.1021/acs.analchem.8b05500
Anal. Chem. 2019, 91, 3078−3084

exclusion step (HiLoad 16/600 Superdex 200 pg column from GE Healthcare) was used to further purify the protein in 10 mM Tris-HCl, pH 8.0, 150 mM NaCl, and 1 mM DTT buffer. The overall yield of the GST-tagged YTH domains was 16−22 mg per 1 L of culture.

The expression and purification of the full length METTL3−METTL14 in SF9 insect cells was carried out as previously described.[13] For improving the METTL3−METTL14 activity, we included 100 μM $ZnCl_2$ in the dialysis buffer to replace possible nickel ions bound to the zinc fingers from the HisTrap FF crude column. The plasmid of $ALKBH5_{74-294}$ with an N-terminal His_6 tag and TEV (Tobacco Etch Virus) protease cleavage site was a gift from Cheryl Arrowsmith (Addgene plasmid # 58754). $ALKBH5_{74-294}$ protein was overexpressed in Rosetta (DE3) cells upon induction with 200 μM IPTG for 20 h at 20 °C. The harvested cells were resuspended in lysis buffer (100 mM Tris-HCl, pH 8.0, 500 mM NaCl) and lysed by sonication. The lysate was centrifuged at 18 000 rpm at 4 °C for 1 h. The soluble fraction was then loaded onto the HisTrap FF crude column (GE Healthcare) and washed with lysis buffer supplemented with 50 mM imidazole. Imidazole (250 mM) in 100 mM Tris-HCl, pH 8.0, and 500 mM NaCl buffer was used to elute the protein. Recombinant TEV protease cleaved the His_6 tag during overnight dialysis at 4 °C against 100 mM Tris-HCl, pH 8.0, and 500 mM NaCl buffer. The dialyzed sample was passed through the HisTrap FF crude column to remove His_6-tagged TEV protease and uncleaved protein. In the final step, the size-exclusion HiLoad 16/600 Superdex 200 pg column (GE Healthcare) further purified the protein in 20 mM Tris-HCl, pH 8.0, supplemented with 150 mM NaCl and 1 mM DTT. Each enzyme was aliquoted and stored at −80 °C until use.

METTL3−METTL14 Assay. The two-step protocol of the METTL3−METTL14 assay consists of a reaction step and subsequent detection step. In the reaction step, active METTL3−METTL14 methylates the 5′-biotinylated single-strand (ss) RNA (5′-AAGAACC**GGACU**AAGCU-3′ purchased from Dharmacon). This reaction was carried out at room temperature in 20 mM Tris-HCl, pH 8.0, supplemented with 0.01% (m/v) bovine serum albumin (BSA). The cosubstrate SAM (Cisbio, 62SAHZLD) was added as the last component and thus initiated the methylation reaction. The intensity of the specific signal for the enzymatic reaction correlates linearly with the enzyme concentration (Figure 2). A good compromise between enzyme usage and signal intensity was determined at a 20 nM concentration of METTL3−METTL14 complex. The reaction progression at 20 nM METTL3−METTL14 was linear up to 40 min. At this fixed time point, the reaction was stopped by the detection buffer (100 mM HEPES, pH 7.5, 300 mM NaCl, 200 mM KF, 0.2% (m/v) BSA), which contains a sufficient amount of salt to inhibit the enzyme activity. The HTRF reagents and m^6A reader proteins can be premixed in detection buffer and can be added simultaneously for stopping the reaction and capturing the methylated product. The final concentrations of anti-GST Eu^{3+}-labeled antibody (Cisbio, 61GSTKLB) and GST-tagged m^6A readers were 0.8 and 25 nM, respectively. In contrast to the constant concentration of HTRF donor, the concentration of XL665-conjugated streptavidin (Cisbio, 610SAXLB) was adjusted to maintain the ratio of 1:8 to the biotinylated RNA. This constraint ensures that the detection portion remains constant in the titration of RNA. The reaction volume was 20 μL, unless stated otherwise. The addition of the detection buffer containing all HTRF reagents and m^6A reader doubled the volume to 40 μL. Capture of the m^6A-modified RNA by the m^6A reader was allowed to proceed for 3 h before the TR-FRET signal was measured using the Infinite M1000 plate reader (Tecan). The plate reader recorded with a delay of 60 μs the emission at 620 and 665 nm after the excitation of the HTRF donor with UV light at 317 nm. This time-resolved measurement eliminates the short-lived background fluorescence of the signal. The emission signal is read over an integration time of 500 μs. The ratio of 665/620 nm signals (HTRF ratio) allows correction for well-to-well variations and media absorbency by colored compounds.[29,30]

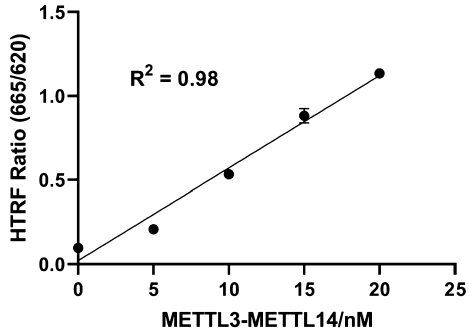

Figure 2. Linear relationship between METTL3−METTL14 concentration and HTRF ratio. The reaction, i.e., first step of the homogeneous time-resolved fluorescence (HTRF)-based assay, was carried out with five different concentrations of METTL3−METTL14 (0, 5, 10, 15, and 20 nM). SAM and unmethylated RNA substrate were kept at 500 and 50 nM, respectively. The detection step was performed with the $YTHDC1_{345-509}$ reader at a concentration of 25 nM. The data points are displayed as the average of duplicates. Error bars in this and the following figures are standard deviations, which are frequently not visible, because they are smaller than the circle used for the average. Note that the data points are HTRF ratios, which are marginally influenced by well-to-well variability.

ALKBH5 Assay. The ALKBH5 assay also comprises a two-step protocol. In the first step, active ALKBH5 demethylates m^6A-containing 5′-biotinylated ss-RNA from Dharmacon. The RNA had an identical sequence to the polynucleotide in the METTL3−METTL14 assay. The reaction was carried out in reaction buffer (50 mM HEPES, pH 7.5, 150 mM NaCl, 0.1% (m/v) BSA, 100 μM $FeSO_4$, 500 μM sodium L-ascorbate) at 37 °C for 1 h. In all of the experiments, the m^6A-containing RNA was kept at 200 nM, while the 2OG was the last component added (the initiator). The reaction volume was 60 μL, from which 15 μL was added to 45 μL of a mixture of HTRF reagents and GST-tagged $YTHDF2_{383-579}$. This solution was prepared in the detection buffer (50 mM HEPES, pH 7.5, 150 mM NaCl, 200 mM KF, 1 mM EDTA, and 0.1% (m/v) BSA). EDTA was included to inhibit the demethylase reaction. The reader $YTHDF2_{383-579}$ at 25 nM captured the m^6A-containing substrate. The HTRF signal was generated by the two fluorophores, Eu^{3+}-labeled antibody and XL665-conjugated streptavidin, which were used at 0.8 and 6.25 nM, respectively. The reagents were allowed to equilibrate for 1 h before the plate reader collected the signals as described above.

DOI: 10.1021/acs.analchem.8b05500
Anal. Chem. 2019, 91, 3078−3084

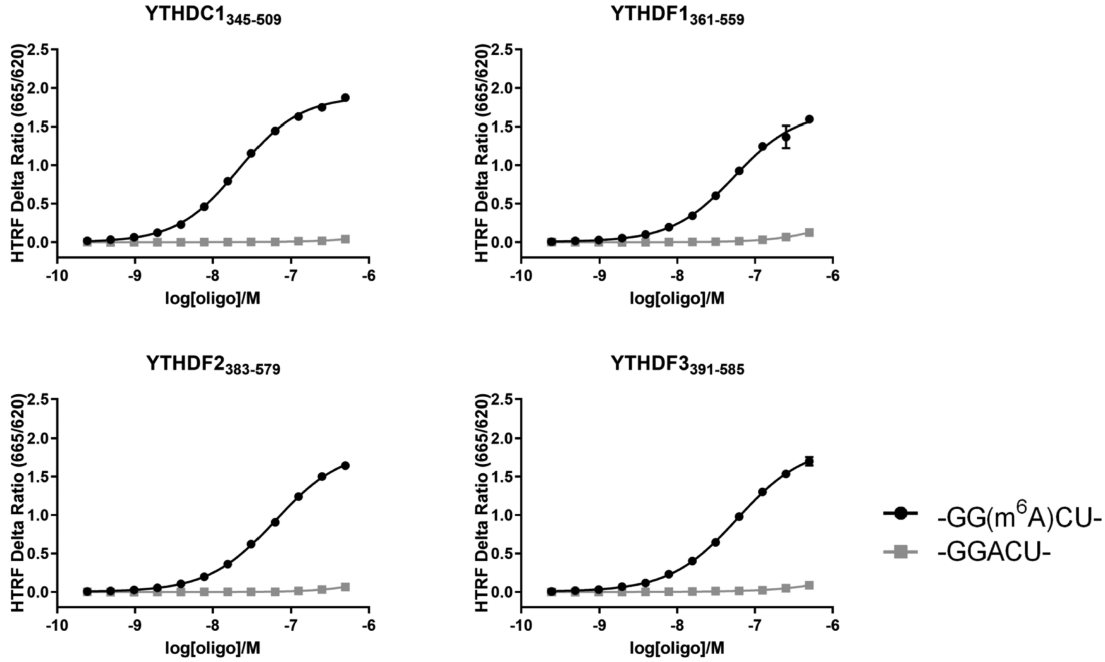

	$YTHDC1_{345-509}$	$YTHDF1_{361-559}$	$YTHDF2_{383-579}$	$YTHDF3_{391-585}$
EC_{50} (nM)	22	56	66	62
Hill slope	1.1	1.1	1.0	1.0

Figure 3. Analysis of sensitivity and specificity of the m^{6}A readers. The titration experiments reveal the sensitivity of m^{6}A readers for m^{6}A methylated RNA and the lack of cross-reactivity for unmodified RNA. The RNA carried the sequence 5′-AAGAACC**GGACU**AAGCU-3′ and was either methylated or unmethylated within the GGACU site. Each m^{6}A reader ($YTHDC1_{345-509}$, $YTHDF1_{361-559}$, $YTHDF2_{383-579}$, $YTHDF3_{391-585}$) was used at a final concentration of 25 nM. HTRF technology detects the RNA−protein binding in the detection buffer (50 mM HEPES, pH 7.5, 150 mM NaCl, 100 mM KF, 0.1% (m/v) BSA) after 2 h of incubation. The HTRF signal is the ratio of acceptor/donor emission (665 nm/620 nm) recorded with a delay of 60 μs after excitation at 317 nm. The ratio of 1:8 between XL665-conjugated streptavidin and biotinylated RNA was maintained. Values of EC_{50} and the Hill slope are shown for the titration with −GG(m^{6}A)CU−. The data points acquired with the unmethylated RNA give no reasonable fitting. The data points are displayed as the average of duplicates.

RESULTS

Sensitivity and Specificity of m^{6}A Readers. We first investigated the detection sensitivity and cross-reactivity. The sensitivity can be quantified by the concentration of methylated RNA at half-maximal HTRF signal (EC_{50}). The cross-reactivity is due to nonspecific interaction between m^{6}A readers and unmethylated RNA. Both properties are assessed by titration experiments using the same RNA oligonucleotide either methylated or unmethylated (Figure 3). In these titrations, the portion of the detected RNA remained constant, since the ratio of 1:8 between XL665-conjugated streptavidin and biotinylated RNA was maintained. This constraint prevents the RNA from exceeding the binding capacity of the system, the so-called "hook" effect.[31] Interestingly, the four m^{6}A readers employed in this study are highly sensitive to the m^{6}A-containing RNA with EC_{50} values of 22 nM for YTHDC1 and around 60 nM for the YTHDF1/2/3. The higher sensitivity of YTHDC1 might originate from differences in a few residues in the binding site as reported for YTHDC1 and YTHDF1.[23] The detection system is suitable for combination with the methylase reaction catalyzed by METTL3−METTL14, since the amount of methylated product falls in the given dynamic range (see below). The dynamic range defines the degree of saturation of the detection system in the linear range of the curve (EC_{10}−EC_{90}). At a concentration above the EC_{85}, the m^{6}A readers start to slightly cross-react with the unmethylated RNA. The level of RNA should, therefore, be below the EC_{85} to keep the background as low as possible. Moreover, the Hill slope close to 1.0 indicates noncooperative binding between m^{6}A-containing RNA and m^{6}A readers.

METTL3−METTL14 Assay. For the assay development, we took into account that the optimal buffer systems for the METTL3−METTL14 reaction and the detection system are different. In this context, we added a doubly (2×) concentrated detection buffer to the optimal buffer for the METTL3−METTL14 reaction. The buffer directly inhibited the reaction by its salt content. Subsequent titration of the unmethylated RNA gives the concentration that preserves the maximal enzyme activity over the reaction time. This titration was carried out at 1 μM SAM. We used YTHDC1 and YTHDF2 to test if the m^{6}A-modified RNA falls into both dynamic ranges (Figure 4A,B).

The amount of substrate and cosubstrate in the assay depends on the purpose in the inhibitor screening. Inhibitors could compete either with RNA or with SAM. The identification of hits from both types requires concentrations of both substrates close to the EC_{50} (i.e., apparent Michaelis−Menten constant (K_m^{app})). Therefore, the biotinylated RNA was used at 50 nM (~EC_{50}) hereafter. We then investigated the effect of the concentration of SAM on the METTL3−METTL14 activity by a titration experiment (Figure 4C). The obtained K_m^{app} value of 59 nM is consistent with the

DOI: 10.1021/acs.analchem.8b05500
Anal. Chem. 2019, 91, 3078−3084

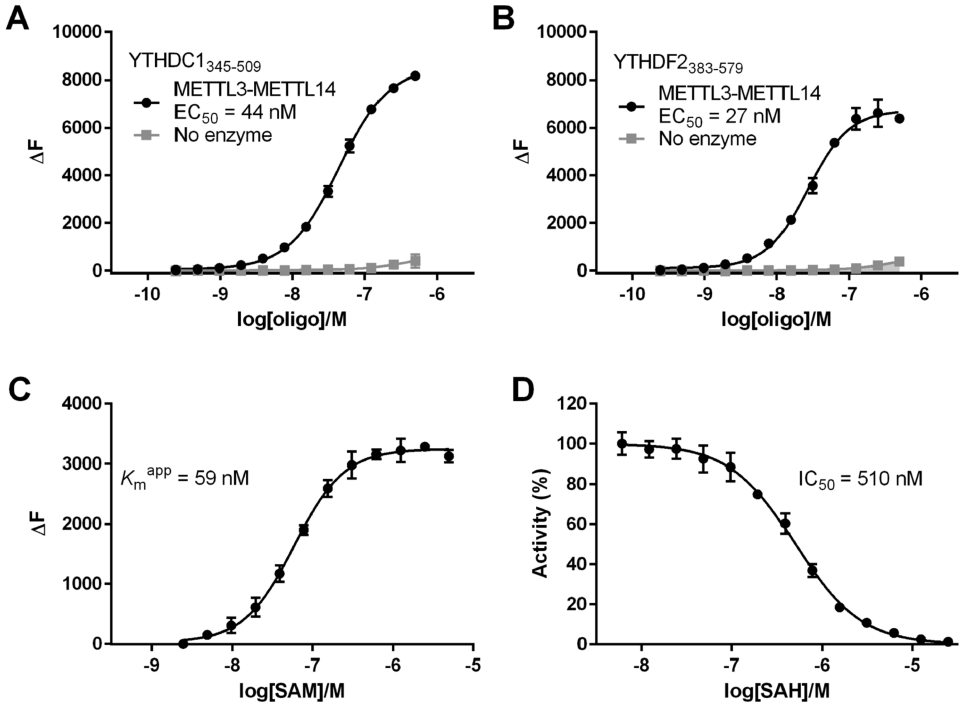

Figure 4. Enzymatic activity of the writer METTL3−METTL14. Unmethylated RNA, the substrate of METTL3−METTL14, was serially diluted against 20 nM enzyme and 1 μM SAM or against 1 μM SAM. The reader domain YTHDC1$_{345-509}$ (A) or YTHDF2$_{383-579}$ (B) captured the m^{6}A-modified product. (C) The apparent Michaelis−Menten constant (K_m^{app}) of SAM was determined with 50 nM RNA. (D) The dose−response curve of SAH, which is a product inhibitor, was carried out using 150 nM SAM and 50 nM RNA. The half-maximal inhibitory concentration (IC$_{50}$) was derived from the fitting of the data points by the nonlinear regression function supplied in GraphPad Prism version 8.00 for Windows. The methylation levels in (C) and (D) were recognized by the reader YTHDC1$_{345-509}$. All of the data points are shown as an average of two independent measurements performed each in duplicates. The ΔF ($\frac{\text{ratio}_{\text{sample}} - \text{ratio}_{\text{background}}}{\text{ratio}_{\text{background}}} * 100$) suppresses the plate-to-plate variation of the two measurements using their background (without SAM) as an internal control.

reported value (102 nM).[20] In the case of SAM, the concentration was set to 2.5 times higher than the K_m^{app} (150 nM) to keep a suitable assay window (i.e., signal/noise) of 9.8. The sensitivity of this platform was evaluated by SAH, which is a byproduct of the SAM-dependent reaction. SAH inhibits the HTRF signal in a concentration-dependent manner with an IC$_{50}$ of 510 nM (Figure 4D). This value is similar to the IC$_{50}$ of 900 nM retrieved from a radioactivity-based assay.[20]

We have also assessed the robustness of our assay in a HTS setup. Using a 384-well microplate, YTHDC1 as reader, and a liquid handler we have obtained a Z'-factor of 0.74 (Figure 5), which is similar to the Z'-factor reported for the radioactivity-based assay (0.78).[20] The Z'-factor reflects the assay dynamics and the data variation, whereby a value between 0.5 and 1 defines a suitable platform for HTS.[32]

ALKBH5 Assay. The demethylation reaction of ALKBH5 decreases the HTRF signal. In this context, the signal without the enzyme was considered as the background. The activity of ALKBH5 depends on ferrous iron, which was at the optimal concentration in the reaction. Surprisingly, the iron slightly interfered with the detection system. As a consequence, the reaction mix was diluted 4 times to reduce the iron concentration in the detection step. The optimal enzyme concentration results from titration experiment at a saturating concentration of 2OG (100 μM, Figure 6A). We selected an enzyme concentration of 200 nM (~EC$_{90}$), which suppresses the signal. The K_m^{app} of 2OG was derived from the titration experiment with 200 nM ALKBH5 (Figure 6B). The K_m^{app} of 1.7 μM for 2OG is consistent with the value derived from a radioactivity-based assay (2 μM).[20] We conclude that the HTRF-based assay with m^{6}A reader can be used to measure the activity of demethylase inhibitors.

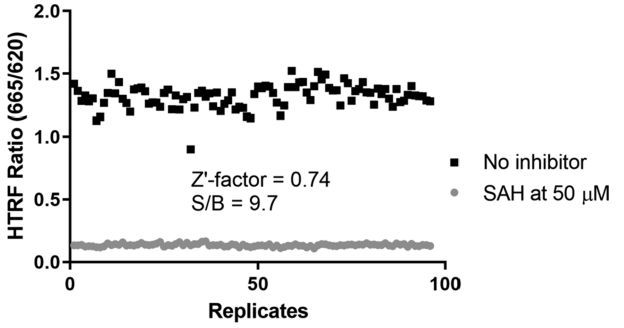

Figure 5. High-throughput compatibility. The methylase reaction catalyzed by METTL3−METTL14 was carried out in 10 μL and 96 replicates. All reagents were dispensed into a white 384-well microplate (Corning, 4513) using a liquid handler (Crystal Gryphon LCP, ARI-Art Robbins Instruments). The concentration of SAM and unmethylated RNA were 150 and 50 nM, respectively. Every second well contained SAH at 50 μM, which acts as inhibitor of the METTL3−METTL14 methylase. The subsequent addition of a mixture of HTRF reagents and the YTHDC1$_{345-509}$ doubled the well volume to 20 μL. The Z'-factor was derived from $1 - \frac{3(\sigma_e + \sigma_{SAH})}{|\mu_e - \mu_{SAH}|}$, where σ and μ are the standard deviation and the mean, respectively, and the subscript e indicates the enzyme reaction without inhibition. The average of the data points of inhibition (B) and no inhibition (S) gives the assay window ($S/B = \mu_e/\mu_{SAH}$).

DOI: 10.1021/acs.analchem.8b05500
Anal. Chem. 2019, 91, 3078−3084

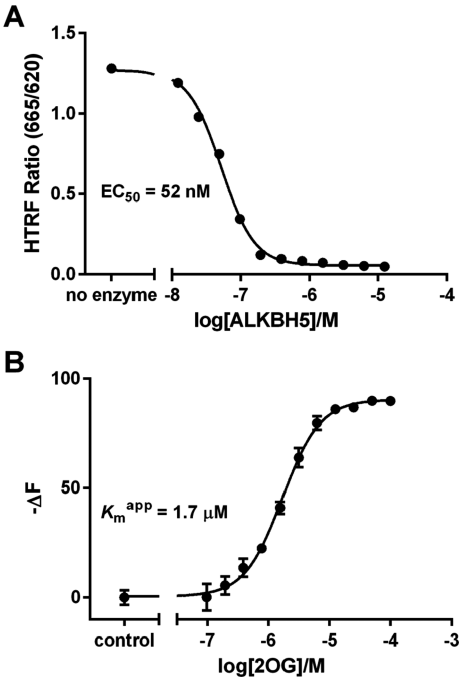

Figure 6. Enzymatic activity of the eraser ALKBH5. (A) Optimal enzyme concentration was determined by titrating the recombinant $ALKBH5_{74-294}$ against m^6A-containing RNA and 100 μM 2-oxoglutaric acid (2OG). $YTHDF2_{383-579}$ captured the rest of m^6A-containing substrate after the demethylation reaction. (B) The apparent Michaelis–Menten constant (K_m^{app}) of 2OG was obtained in the presence of 200 nM $ALKBH5_{74-294}$. ΔF is calculated as described in Figure 4. The data points are displayed as an average of duplicates from a single measurement in (A) and two independent measurements performed each in duplicates in (B).

CONCLUSION

We have proposed a novel HTRF-based detection system for the sensitive and specific quantification of m^6A-modified RNA, the product or substrate of the reaction catalyzed by METTL3–METTL14 or ALKBH5, respectively. The assay takes advantage of the human m^6A readers as analytical tools for the detection of m^6A in the context of specific RNA sequences, in contrast to m^6A-specific antibodies, typically raised against the isolated N^6-methyladenosine.[33,34] The highly robust assay can be used in screening of inhibitors of the methylase METTL3–METTL14 and demethylase ALKBH5. Since recent evidence suggests that m^6A readers bind also to m^1A,[26] the assay can be adapted to m^1A modification. Compared with previously reported methods, our reader-based assay does not suffer from impractical disadvantages like radioactive labeling, multiple washing steps, and/or the use of special instruments. Notably, the consumption of enzyme and substrates is low, and the assay can be used in high-throughput format.

AUTHOR INFORMATION

Corresponding Authors

*E-mail: p.sledz@bioc.uzh.ch (P.Ś.)
*E-mail: caflisch@bioc.uzh.ch (A.C.)

ORCID

Amedeo Caflisch: 0000-0002-2317-6792

Notes

The authors declare no competing financial interest.

ACKNOWLEDGMENTS

We thank Beat Blatmann for help with the setup of the liquid handler. This work was supported financially by a grant of the Swiss National Science Foundation to A.C. and a grant from UZH Bioentrepreneurship Program to P.Ś.

REFERENCES

(1) Wei, C. M.; Gershowitz, A.; Moss, B. *Cell* **1975**, *4*, 379–386.
(2) Narayan, P.; Rottman, F. M. *Science (Washington, DC, U. S.)* **1988**, *242*, 1159–1162.
(3) Harper, J. E.; Miceli, S. M.; Roberts, R. J.; Manley, J. L. *Nucleic Acids Res.* **1990**, *18*, 5735–5741.
(4) Liu, J.; Yue, Y.; Han, D.; Wang, X.; Fu, Y.; Zhang, L.; Jia, G.; Yu, M.; Lu, Z.; Deng, X.; Dai, Q.; Chen, W.; He, C. *Nat. Chem. Biol.* **2014**, *10*, 93–95.
(5) Meyer, K. D.; Saletore, Y.; Zumbo, P.; Elemento, O.; Mason, C. E.; Jaffrey, S. R. *Cell* **2012**, *149*, 1635–1646.
(6) Dominissini, D.; Moshitch-Moshkovitz, S.; Schwartz, S.; Salmon-Divon, M.; Ungar, L.; Osenberg, S.; Cesarkas, K.; Jacob-Hirsch, J.; Amariglio, N.; Kupiec, M.; Sorek, R.; Rechavi, G. *Nature* **2012**, *485*, 201–206.
(7) Bokar, J. A.; Shambaugh, M. E.; Polayes, D.; Matera, A. G.; Rottman, F. M. *RNA (New York, N.Y.)* **1997**, *3*, 1233–1247.
(8) Jia, G.; Fu, Y.; Zhao, X.; Dai, Q.; Zheng, G.; Yang, Y.; Yi, C.; Lindahl, T.; Pan, T.; Yang, Y.; He, C. *Nat. Chem. Biol.* **2011**, *7*, 885–887.
(9) Zheng, G.; et al. *Mol. Cell* **2013**, *49*, 18–29.
(10) Mauer, J.; Luo, X.; Blanjoie, A.; Jiao, X.; Grozhik, A. V.; Patil, D. P.; Linder, B.; Pickering, B. F.; Vasseur, J.-J.; Chen, Q.; Gross, S. S.; Elemento, O.; Debart, F.; Kiledjian, M.; Jaffrey, S. R. *Nature* **2017**, *541*, 371–375.
(11) Ping, X.-L.; et al. *Cell Res.* **2014**, *24*, 177–189.
(12) Patil, D. P.; Chen, C.-K.; Pickering, B. F.; Chow, A.; Jackson, C.; Guttman, M.; Jaffrey, S. R. *Nature* **2016**, *537*, 369–373.
(13) Śledź, P.; Jinek, M. *eLife* **2016**, *5*, No. e18434.
(14) Wang, P.; Doxtader, K. A.; Nam, Y. *Mol. Cell* **2016**, *63*, 306–317.
(15) Wang, X.; Feng, J.; Xue, Y.; Guan, Z.; Zhang, D.; Liu, Z.; Gong, Z.; Wang, Q.; Huang, J.; Tang, C.; Zou, T.; Yin, P. *Nature* **2016**, *534*, 575–578.
(16) Vu, L. P.; Pickering, B. F.; Cheng, Y; Zaccara, S; Nguyen, D.; et al. *Nat. Med. (N. Y., NY, U. S.)* **2017**, *23*, 1369–1376.
(17) Chen, M.; Wei, L.; Law, C.; Tsang, F. H.; Shen, J.; Cheng, C. L.; Tsang, L.; Ho, D. W.; Chiu, D. K.; Lee, J. M.; Wong, C. C.; Ng, I. O.; Wong, C. *Hepatology* **2018**, *67*, 2254–2270.
(18) Lin, S.; Choe, J.; Du, P.; Triboulet, R.; Gregory, R. I. *Mol. Cell* **2016**, *62*, 335–345.
(19) Boriack-Sjodin, P. A.; Ribich, S.; Copeland, R. A. *Nat. Rev. Drug Discovery* **2018**, *17*, 435–453.
(20) Li, F.; Kennedy, S.; Hajian, T.; Gibson, E.; Seitova, A.; Xu, C.; Arrowsmith, C. H.; Vedadi, M. *J. Biomol. Screening* **2016**, *21*, 290–297.
(21) Huang, J.; Dong, X.; Gong, Z.; Qin, L.; Yang, S.; Zhu, Y.; Wang, X.; Zhang, D.; Zou, T.; Yin, P.; Tang, C. *Protein Cell* **2018**, 1–13.
(22) Imanishi, M.; Tsuji, S.; Suda, A.; Futaki, S. *Chem. Commun. (Cambridge, U. K.)* **2017**, *53*, 12930–12933.
(23) Xu, C.; Liu, K.; Ahmed, H.; Loppnau, P.; Schapira, M.; Min, J. *J. Biol. Chem.* **2015**, *290*, 24902–24913.
(24) Xu, C.; Wang, X.; Liu, K.; Roundtree, I. A.; Tempel, W.; Li, Y.; Lu, Z.; He, C.; Min, J. *Nat. Chem. Biol.* **2014**, *10*, 927–929.
(25) Zhu, T.; Roundtree, I. A.; Wang, P.; Wang, X.; Wang, L.; Sun, C.; Tian, Y.; Li, J.; He, C.; Xu, Y. *Cell Res.* **2014**, *24*, 1493–1496.
(26) Dai, X.; Wang, T.; Gonzalez, G.; Wang, Y. *Anal. Chem.* **2018**, *90*, 6380–6384.
(27) Baltz, A. G.; Munschauer, M.; Schwanhäusser, B.; Vasile, A.; Murakawa, Y.; Schueler, M.; Youngs, N.; Penfold-Brown, D.; Drew,

DOI: 10.1021/acs.analchem.8b05500
Anal. Chem. 2019, 91, 3078–3084

K.; Milek, M.; Wyler, E.; Bonneau, R.; Selbach, M.; Dieterich, C.; Landthaler, M. *Mol. Cell* **2012**, *46*, 674−690.
(28) Wang, X.; Lu, Z.; Gomez, A.; Hon, G. C.; Yue, Y.; Han, D.; Fu, Y.; Parisien, M.; Dai, Q.; Jia, G.; Ren, B.; Pan, T.; He, C. *Nature* **2014**, *505*, 117−120.
(29) Mabile, M.; Mathis, G.; Jolu, E. J.-P.; Pouyat, D.; Dumont, C. Method Of Measuring The Luminescence Emitted In A Luminescent Assay. US 5527684 A, 1996.
(30) Degorce, F.; Card, A.; Soh, S.; Trinquet, E.; Knapik, G. P.; Xie, B. *Curr. Chem. Genomics* **2009**, *3*, 22−32.
(31) Amarasiri Fernando, S.; Wilson, G. S. *J. Immunol. Methods* **1992**, *151*, 47−66.
(32) Zhang; Chung; Oldenburg, J. *J. Biomol. Screening* **1999**, *4*, 67−73.
(33) Bringmann, P.; Lührmann, R. *FEBS Lett.* **1987**, *213*, 309−315.
(34) Munns, T. W.; Liszewski, M. K.; Sims, H. F. *Biochemistry* **1977**, *16*, 2163−2168.

DOI: 10.1021/acs.analchem.8b05500
Anal. Chem. 2019, 91, 3078−3084